

Geochemistry of peridotite xenoliths from the Sverrefjell Volcano, Western Spitsbergen: implications for mantle metasomatism

ABSTRACT

Mantle xenoliths entrained in the Quaternary Sverrefjell volcano from Spitsbergen have been studied with the aim of understanding the nature of metasomatizing agents which affected the subcontinental lithospheric mantle beneath Spitsbergen. The suit of mantle xenoliths consists of spinel lherzolites, spinel harzburgites and websterites. The textures of all three rock types range from protogranular to porphyroclastic. Concentrations of Al_2O_3 , CaO, TiO_2 and Na_2O decrease gradually from websterites through lherzolites to harzburgites. LREE and other incompatible trace elements usually increase from depleted harzburgite to enriched lherzolites and websterites, indicating that metasomatism affected mainly the lherzolites and websterites. However, the exceptions are a few clinopyroxene patterns from harzburgites with mostly enriched LREEs imprinted by metasomatic processes. Clinopyroxenes show highly variable mantle normalized REE patterns but can be classified into four major groups showing: 1) LREE depleted to flat patterns (La_N/Ce_N 0.39-1.26; Ce_N/Yb_N 0.29-0.63; Sm_N/Yb_N 0.75-1.07), 2) spoon-shaped (MREE enriched) REE patterns (La_N/Ce_N 1.26-2.85; Ce_N/Yb_N 1.43-7.74; Sm_N/Yb_N 1.21-2.80), 3) highly enriched LREE and fractionated LREE/HREE patterns (La_N/Ce_N 0.83-1.24; Ce_N/Yb_N 5.57-24.68; Sm_N/Yb_N 1.30-6.60), and 4) LREE enriched and MREE depleted u-shaped patterns (La_N/Ce_N 1.92-2.02; Ce_N/Yb_N 4.53-5.29; Sm_N/Yb_N 0.35-0.49). Type 3 clinopyroxenes show trace element signatures produced by reaction of carbonate-rich fluids. Type 4 clinopyroxenes are significantly enriched in U, Th, Pb, Zr and show U-shaped REE patterns, which may have been caused by subduction-related hydrous fluids or melts. The Sr-Nd-Pb isotopic compositions of clinopyroxenes show a gradual variation from depleted MORB (DMM) type 1 clinopyroxenes to very enriched type 2 and 3 clinopyroxenes.

Regional & sample location map

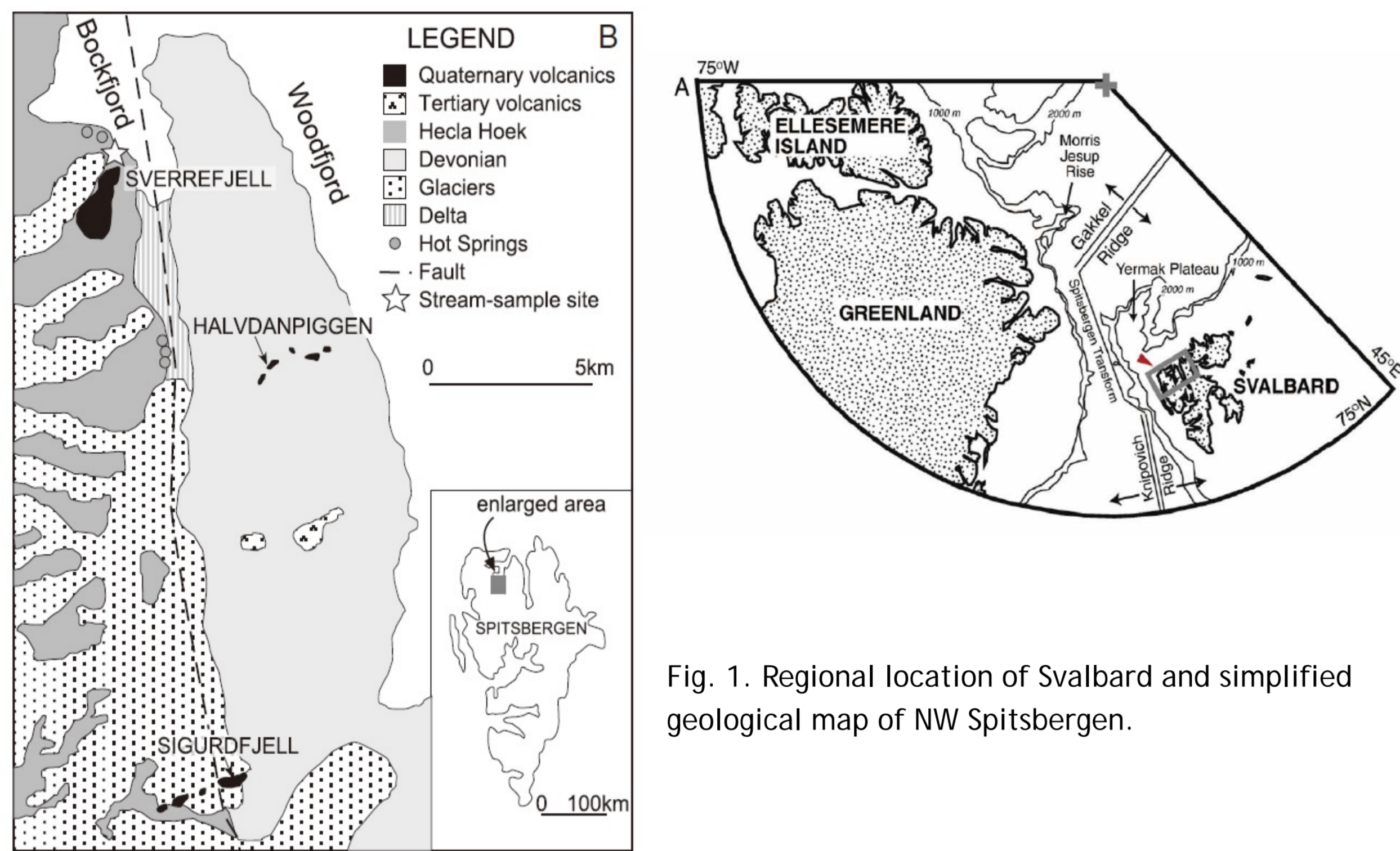


Fig. 1. Regional location of Svalbard and simplified geological map of NW Spitsbergen.

Sverrefjell peridotites

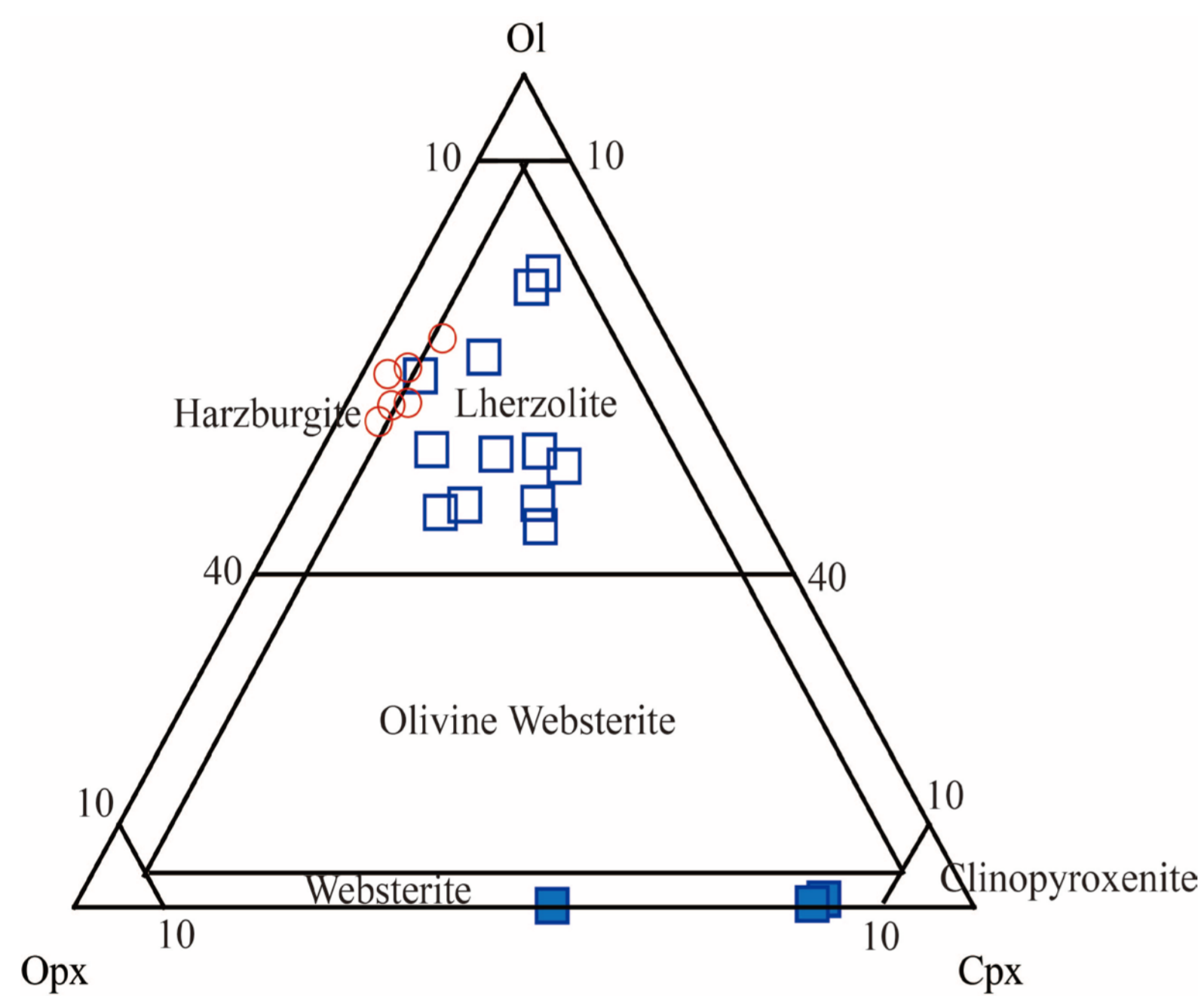


Fig. 2. Olivine-orthopyroxene-clinopyroxene diagram (Le Maitre 2002) for the mantle xenoliths from Sverrefjell volcano, Western Spitsbergen.

Major and trace element compositions of Whole rock peridotites

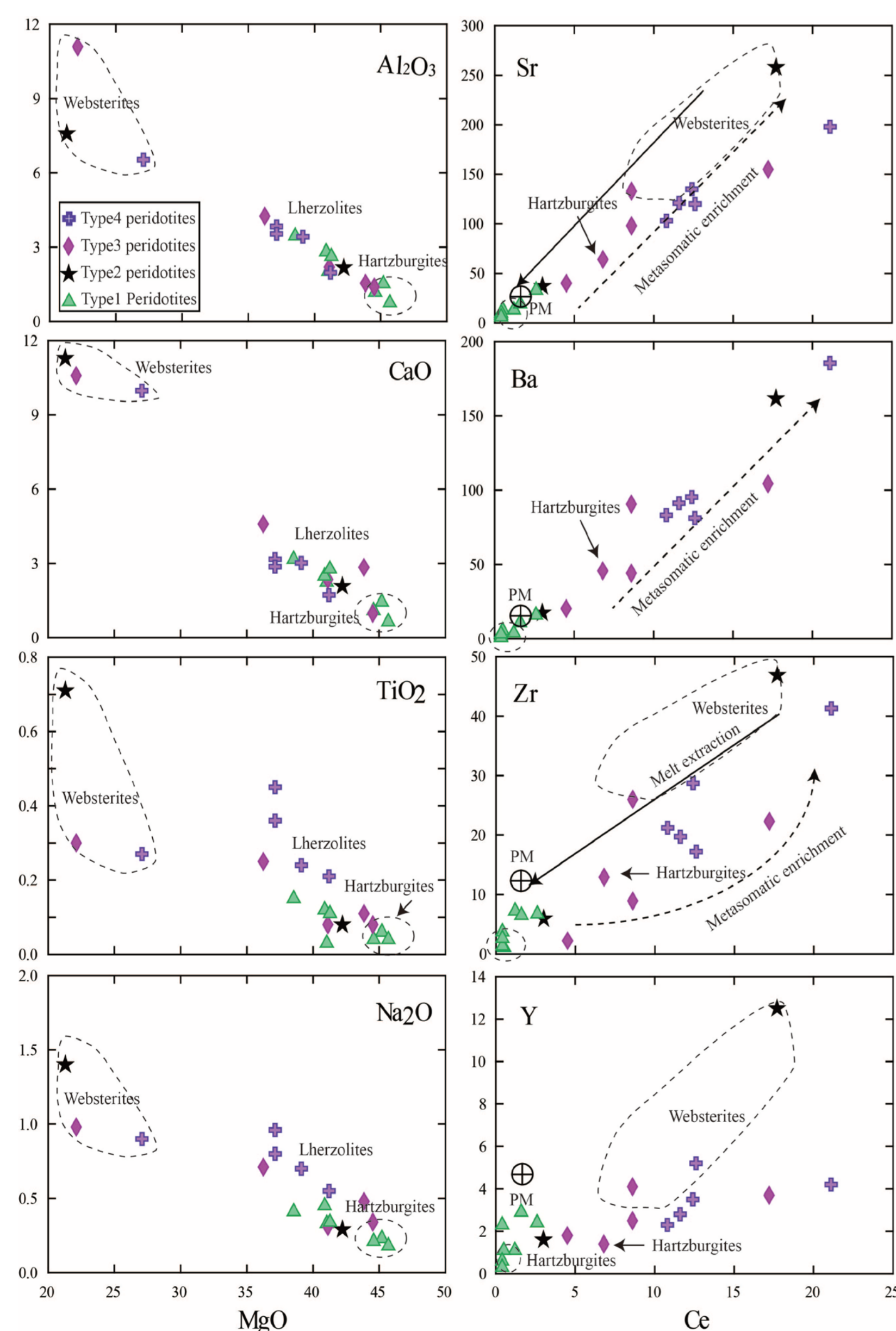


Fig. 3. Co-variation diagrams of Al_2O_3 , TiO_2 , CaO and Na_2O vs. MgO and selected trace elements vs. Ce in peridotites from Sverrefjell volcano, Western Spitsbergen. The peridotites are subdivided into 4 types based on their REE and trace element abundant patterns.

Major compositions of clinopyroxenes

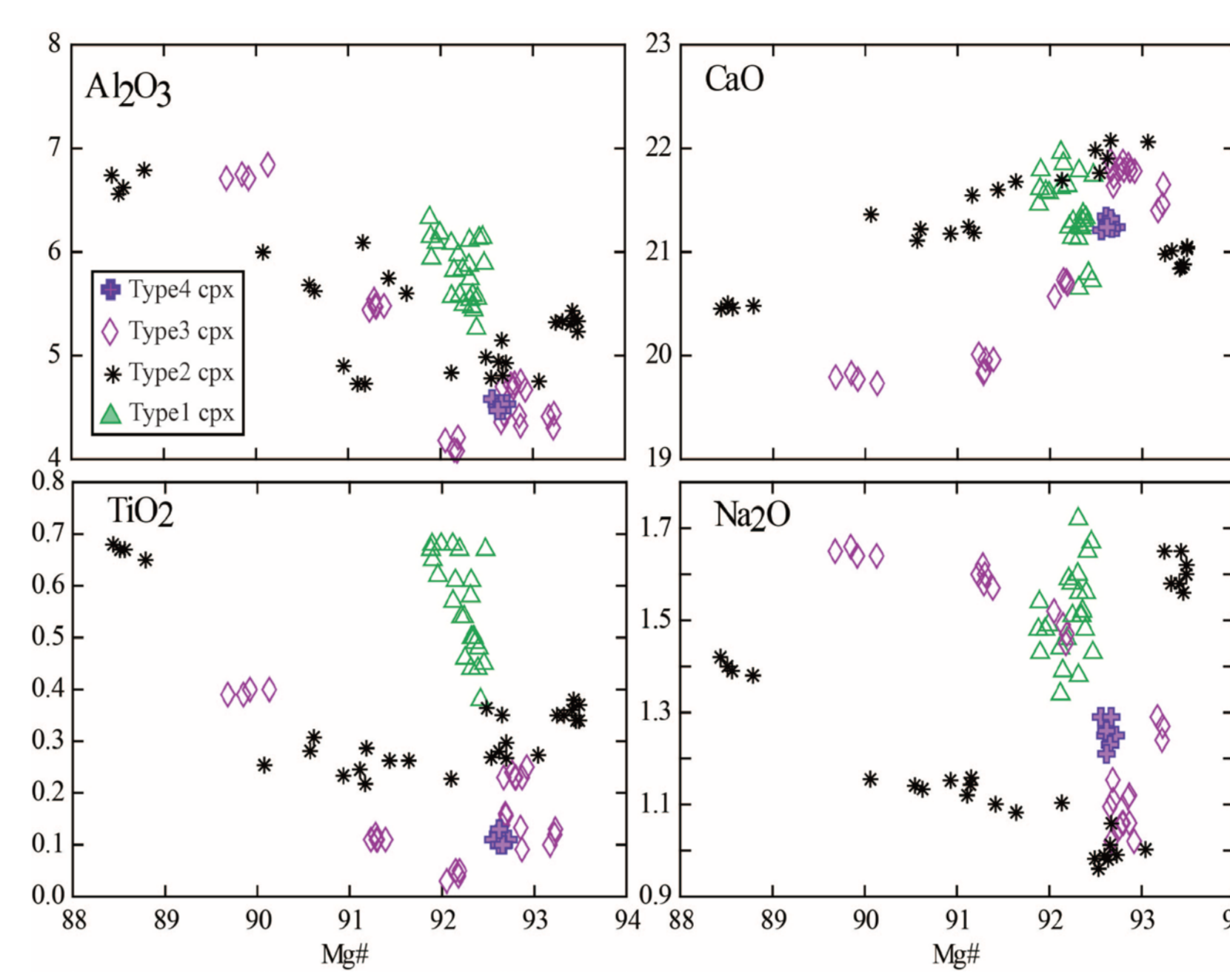


Fig. 4. Variation diagrams of Al_2O_3 , TiO_2 , CaO and Na_2O vs. MgO in clinopyroxenes from Sverrefjell volcano, Western Spitsbergen.

REE abundance patterns

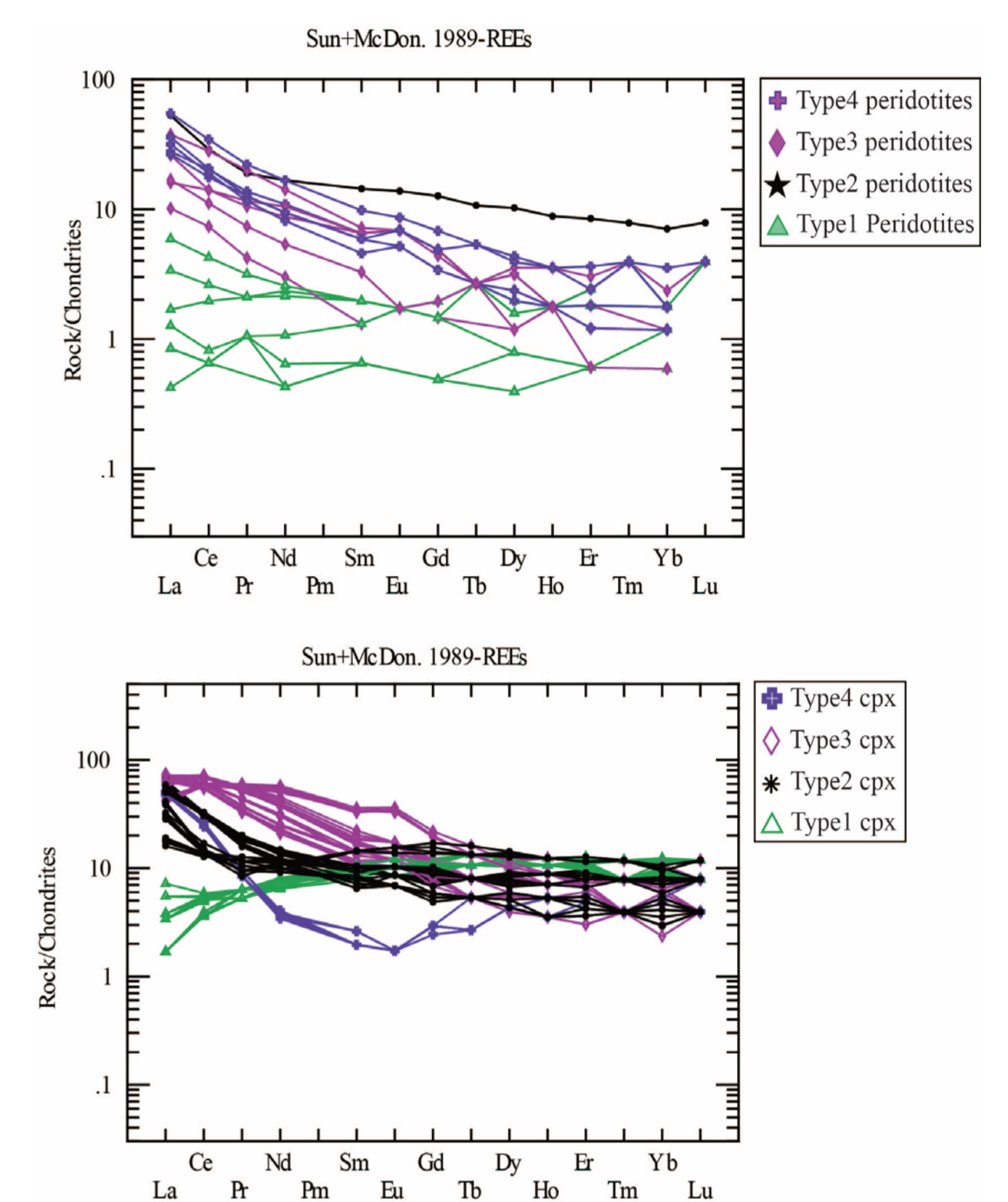


Fig. 5. REE patterns normalized to chondrite for clinopyroxenes and peridotites from Sverrefjell volcano, Western Spitsbergen.

Incompatible trace element compositions of clinopyroxenes

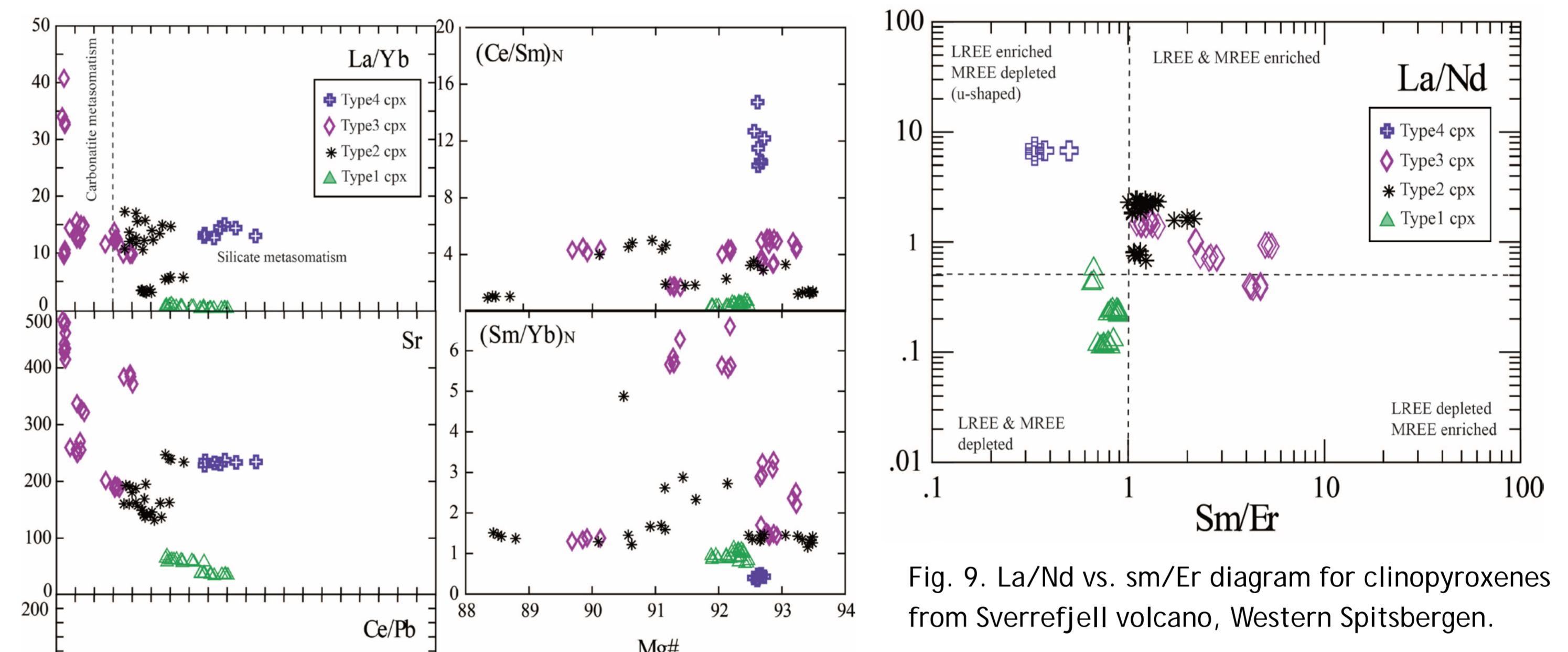


Fig. 6. Trace element variation diagrams in clinopyroxenes from Sverrefjell volcano, Western Spitsbergen.

Sr-Nd-Pb isotopic compositions of clinopyroxenes

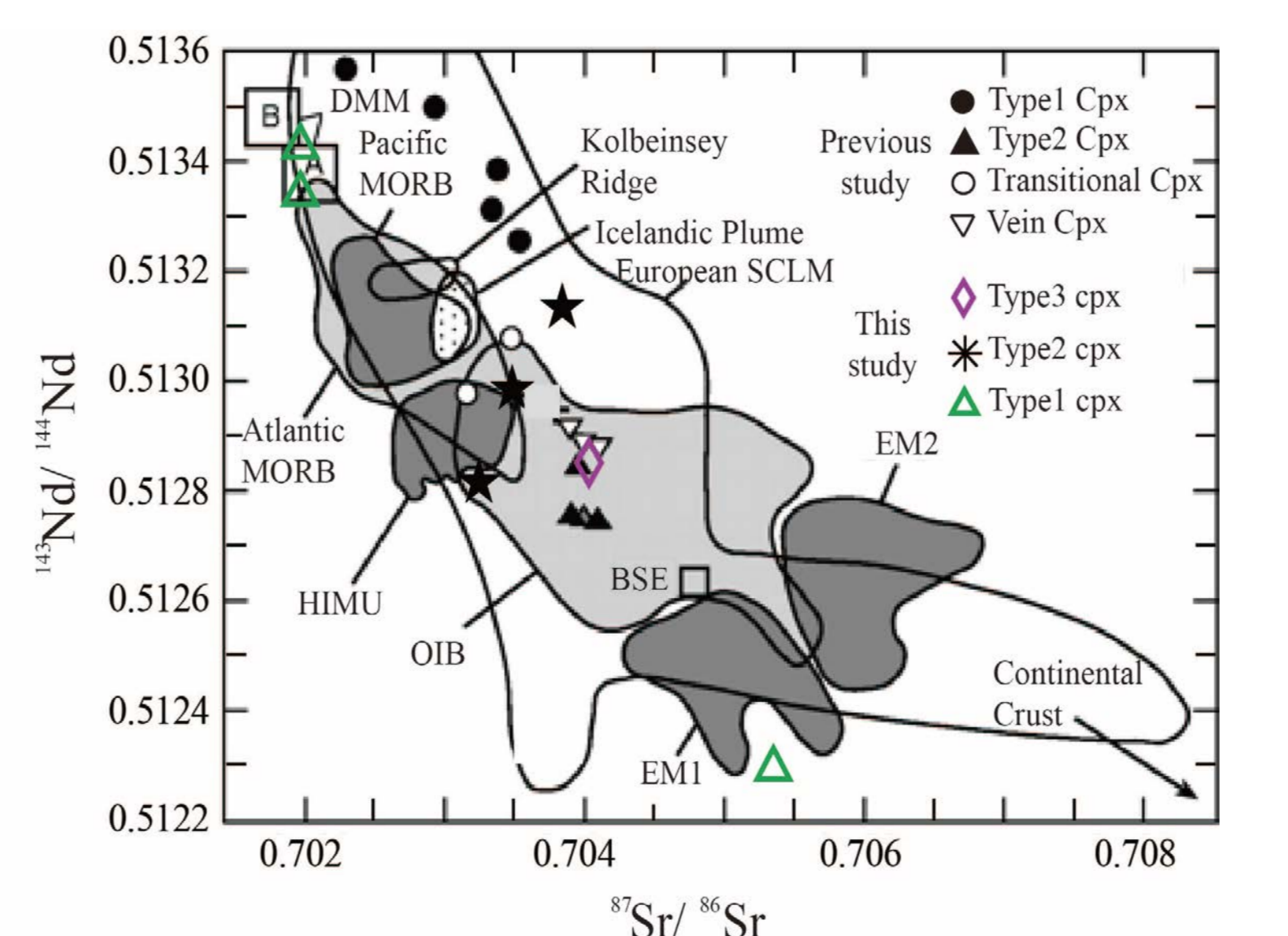


Fig. 7. Sr-Nd isotope variation diagram for peridotites from Sverrefjell volcano, Western Spitsbergen. Data from Ionov et al 2002 are also plotted. The fields of oceanic basalts and model mantle end-members (Zindler & Hart, 1986; Hofmann, 1997), and of European lithospheric mantle (SCLM) (Downes, 2001) are shown. A and B are two distinct DMM fields as defined by Zindler & Hart (1986).

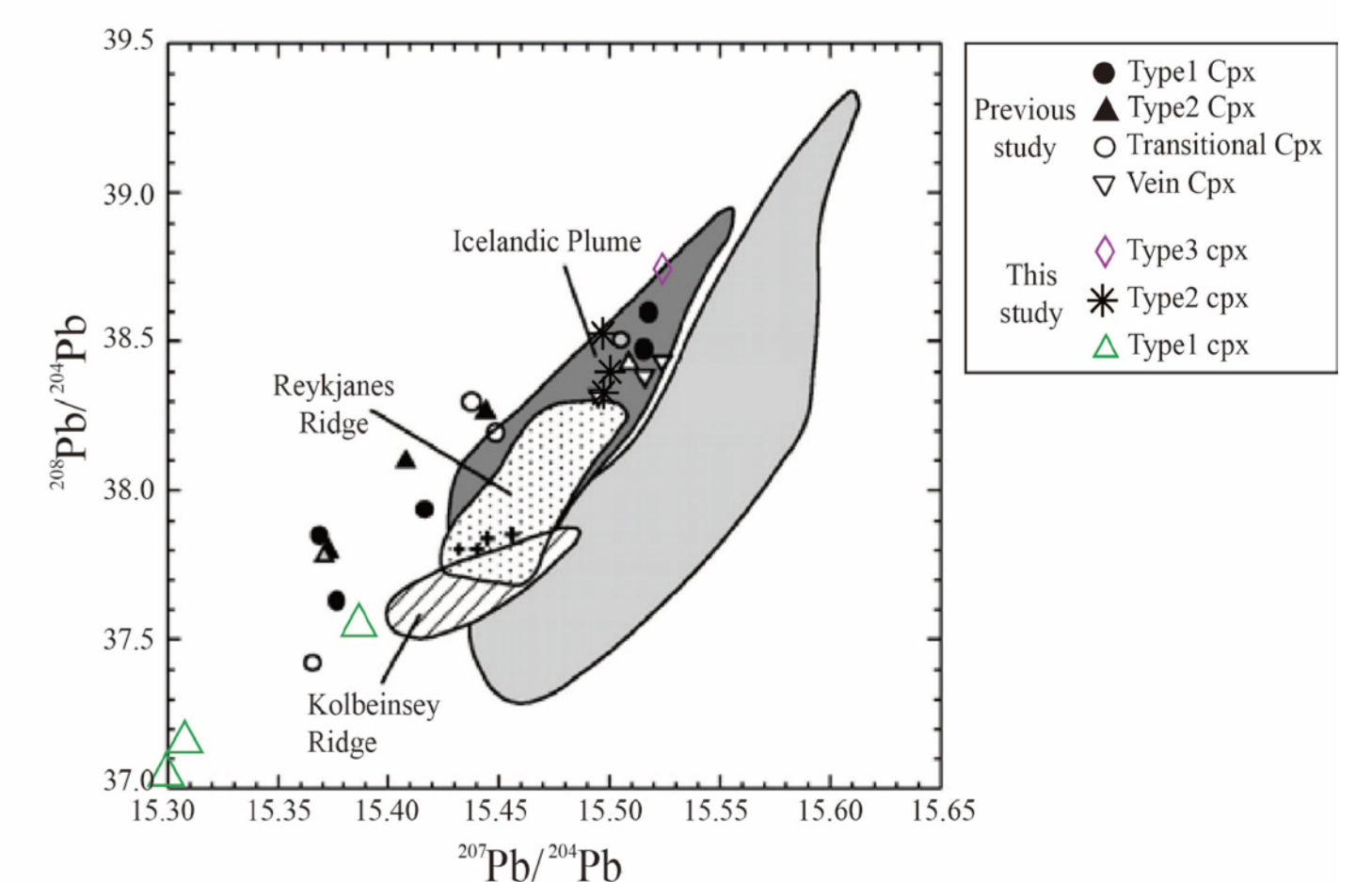


Fig. 8. A plot of $^{208}Pb/^{204}Pb$ vs $^{207}Pb/^{204}Pb$. Also shown are the fields of oceanic basalts in the vicinity of Spitsbergen (Kempton et al., 2000), and plotted the data from Ionov et al (2002).